# IN-SITU CHARACTERIZATION OF K$_2$CsSb PHOTOCATHODES*

M. A. H. Schmeißer[#], A. Jankowiak, T. Kamps, Helmholtz-Zentrum Berlin, Germany
S. G. Schubert, Brookhaven National Lab, Upton, NY, USA

## Abstract

Alkali antimonide photocathodes with high quantum efficiency hold the promise of delivering electrons for high-brightness injectors. A drift type spectrometer (momentatron) was attached to the HZB preparation system to allow in-situ characterization within short time after fabrication and possibly identify correlations between growth process and cathode performance parameters.

## MOTIVATION

SRF photoinjectors for high brightness beams are an enabling technology for next-generation accelerator projects like bERLinPro. They rely on rigid photocathodes with high quantum efficiency for the generation of electron beams with high average currents. K$_2$CsSb cathodes are good candidates for this purpose due to their high QE and fast pulse response. Such cathodes have been prepared with QEs greater than 1% and up to 10% at 532 nm [1, 2] but the details of the growth and the influence of process parameters on the cathode's properties are not well understood. The initial transverse momentum of the electrons emitted from the cathode, which sets a limit for the beam brightness in the accelerator, can be resolved with the momentatron. Additionally, together with surface science characterization techniques [3], this information may provide insight on the influence of structural properties like crystal orientations, crystallite sizes, and stoichiometry of the cathode on the emittance as a figure of merit for accelerator science.

## CATHODE PREPARATION

Alkali-Antimonides are highly reactive materials and exposure to small amounts of residual gases like water, oxygen, and CO can destroy the material or prevent crystallization. Therefore a preparation chamber dedicated for the growth and analysis of alkali antimonide photocathodes was recently developed and built at Helmholtz-Zentrum Berlin (HZB). In an effort to foster an international cooperation on cathode research and development, the whole system was moved to Brookhaven National Lab (BNL) in Upton, NY, USA, where it was commissioned. The samples are prepared in an UHV chamber with a base pressure below $10^{-9}$ mbar that allows physical vapour deposition (PVD) of Potassium, Caesium and Antimony from evaporation sources as shown in figure 2. The alkali metals are evaporated from Alvatec V-sources and the deposition rate is monitored by quartz microbalances.

Below the preparation chamber and separated by a large valve, an analysis chamber is available and the sample can
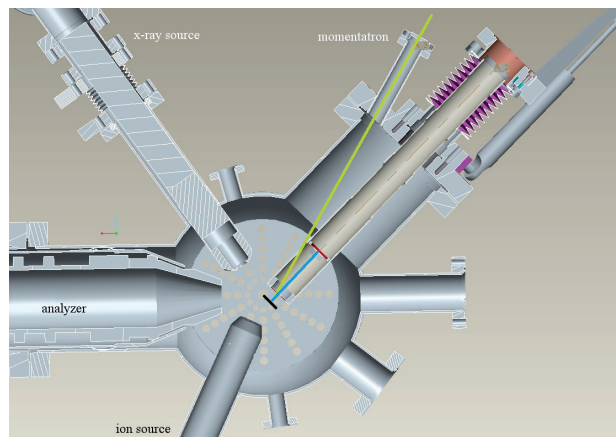
Figure 1: CAD drawing of the momentatron mounted in the analysis chamber mounted in the top right flange. The laser and electron paths are shown as green and blue lines. On the left side in counter clockwise direction an X-Ray source, the electron analyser, and an ion source are mounted.

be transferred without breaking the vacuum. It supports an X-Ray source and a hemispherical electron detector for X-ray photoelectron spectroscopy (XPS) and an ion source for low-energy ion scattering experiments. Additionally, the momentatron is mounted in this chamber. A 3-axis manipulator transfers the sample between the two chambers. The sample holder is electrically isolated and a bias voltage of ±100V can be applied. Resistive heating is available but the heater has electrical contact to the sample, so its controller has to be unplugged for any measurements that require a bias applied to the sample. A Keithley 6517B picoampere-meter is used both as a bias voltage source and to measure the photocurrent.

### Preparation of a Cs$_3$Sb Cathode

During a first measurement campaign, the cathode preparation system was commissioned and a first Caesium Antimonide cathode was prepared. A photocurrent of 10 $\mu$A was obtained from the photocathode. The photocurrent measurement was space charge limited, so only a lower limit of the QE can be reported which is 0.5%. As shown in figure 3, the photocurrent reduced quickly, the 1/e lifetime was estimated to 50 minutes. The potassium source was degassing strongly which compromised the vacuum pressure and prevented the use of this source. For the second campaign improvements of the vacuum system are planned which should shorten the bakeout time and help achieve base pressures below $10^{-9}$ mbar.

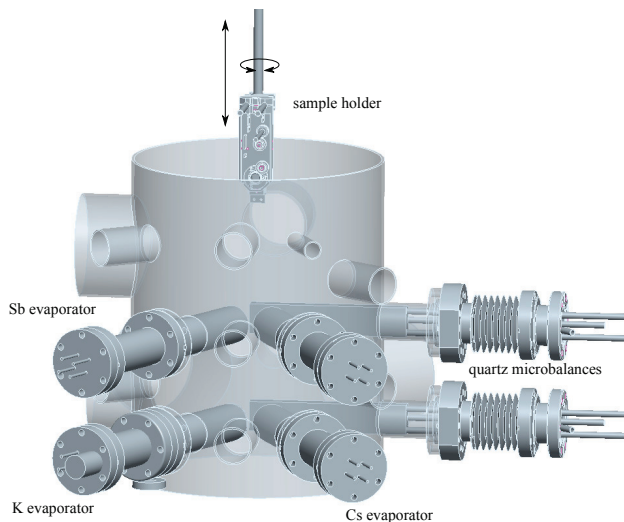**03 Particle Sources and Alternative Acceleration Techniques**

Figure 2: CAD drawing of the preparation chamber of the system. The sample holder, evaporation sources, and quartz monitors are displayed. Vacuum components are omitted for clarity.
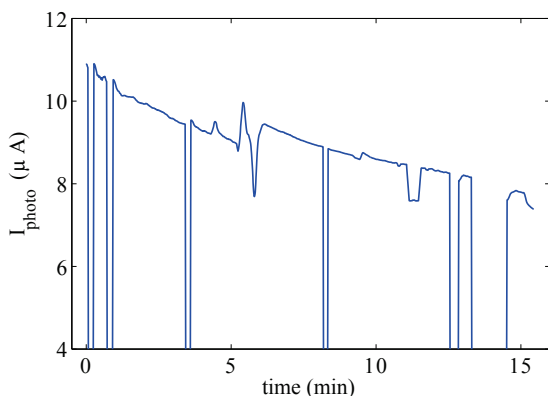


Figure 3: Photocurrent from the $Cs_3Sb$ photocathode under illumination by a 5 mW green laser (532nm) over time. The drops in the signal are from manually blocking the laser light. The wiggle at about 5 minutes is due to a movement of the laser spot on the sample surface.

## MOMENTATRON

The momentatron is a device that allows measurement of the intrinsic transverse momentum distribution of an electron beam emitted from a photocathode. It was developed and mounted to the photocathode preparation and analysis chamber where it will be used to perform in-situ diagnostics of the prepared cathodes without exposure to ambient conditions. The goal is to find correlations between cathode preparation parameters and the transverse momentum distribution. Figure 4 provides an illustration of the working principle and a photograph of the momentatron.

The electrons are emitted from a small laser-illuminated spot on the cathode sample. After acceleration in a short gap $g$ between the sample and a mesh, they are allowed to drift in

a field free region $d$. A copper mesh with 18x18 $\mu$m square holes and 1000 lines per inch is used. The electrons are detected by a scintillating screen which is imaged by a CCD camera. The radial coordinate $r$ at the position of the screen depends linearly on the intrinsic transverse momentum $p_x$

$$\frac{p_x}{mc} = \frac{r}{2g + d} \sqrt{\frac{2eU}{mc^2}} , \qquad (1)$$

and a radial distribution of $p_x$ can be obtained from the radial intensity distribution on the screen. Here, $p_x$ is expressed in units of $mc$ (electron mass times speed of light), $e$ is the elementary charge and $U$ is the potential difference between sample and grid.
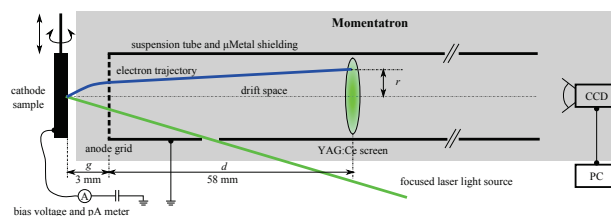




Figure 4: Schematic illustration of the working principle of the momentatron (top) and photograph of the device (bottom).

Design parameters of the system are the gap and drift distances and the applied bias voltage, as well as type and material of the grid and scintillation screen. The drift distance was optimized to obtain maximum resolution of the electron beam on the screen, while the accelerating voltage was limited to -100 V by the electrical isolation of the available sample holder.

To minimize influence of the earth magnetic field and possible stray field from the pumps, the drift region is shielded by high-$\mu$ material. The flatness of the accelerating field depends on the angle between the cathode sample and the anode grid, which is ideally zero but cannot be measured directly in the experiment. Finite-element simulations predict that the electron beam is only steered but the transverse distribution is not distorted when the angle is below 5 deg. Figure 5 shows the beam center and rms widths of the left and right hand sides of a gaussian beam emitted from a 100 $\mu$m spot. Possibly the sample can be positioned by beam based alignment [4]. A systematic error is introduced by the spot size of the laser light, which can be estimated by reproducing the optical path and corrected for. Additional uncertainties arise from the lens effect of the grid, a local curvature (folds) in the grid mesh, the uncertainty of the gap length, and the point spread function of the scintillator. The folds of the grid introduce the largest error of 2 % at the expected transverse energies. All discussed errors are listed in table 1, error

Table 1: Sources of Error in the Transverse Momentum Measurement

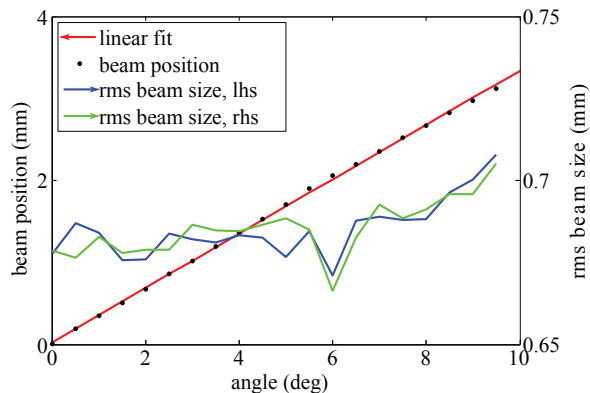| | resolution limit | voltage dependence | magnitude $\Delta r$ | rel. error on $p_x$ |
|---|---|---|---|---|
| E field | $\frac{Dd}{4g}$ | $d \propto \sqrt{U}$ | $84\,\mu m$ | 1% |
| angle & mesh | $\tan(0.5°)d$ | $\sqrt{U}$ | $145\,\mu m$ | 2% |
| $\Delta d$ (gap) | $\frac{\Delta p_x}{mc} \approx \frac{2r}{d^2}\sqrt{\frac{2eU}{mc^2}}$ | $1/\sqrt{U}$ | $\frac{\Delta p_x}{mc} \sim 5 \cdot 10^{-6}$ | 1% |
| imaging | aperture | - | $8\,\mu m$ | 0.1% |



Figure 5: Influence of an angle between anode and cathode. For small angles, the beam position is steered linearly and the rms width on the left and right hand side stay constant. The slope of the steering is 330 $\mu$m per degree angle.

addition results in a total relative uncertainty of 3 % for the transverse momentum. The setup is currently mounted in the analysis chamber of the system and will be used for cathode characterization in future.

*Imaging and Data Acquisition*

The detection of the electrons will be performed by a cerium doped YAG screen that is monitored by a CCD camera (Basler scout sc640-74gm). The light output (emitted photons per incident electron) for low energy electrons is unknown but expected to be about 50 % from extrapolation of high energy data [5]. At 10 $\mu$A photocurrent, on average about $2 \cdot 10^5$ photons reach a single pixel per second through the lens aperture. Assuming a 50 % quantum efficiency of the CCD chip, the exposure time should be about 250 ms to reach the saturation capacity of $2.5 \cdot 10^4$ electrons per pixel. In order to acquire images from the camera, either MATLAB or a custom C++ program is used. A graphical user interface allows convenient monitoring of the camera data and displays histograms and Gaussian fits of the data. The MATLAB implementation proved to be convenient for final data analysis and archival which is also performed in MATLAB.

The intensity distribution of electrons at the screen position is represented as a 2D image from the CCD camera. The radial intensity distribution is reconstructed by azimuthally integrating the acquired data. The intensity value of each pixel is assigned to bins that are formed by concentric circles of equal distance around the center of gravity. The bins are normalized to their area and then yield the radial distribution in arbitrary units with respect to the distance to the center of gravity. Background noise from the CCD chip is efficiently suppressed by subtracting a dark image and averaging over the circle (bin) area. A Gaussian test distribution can well be recovered at signal to noise amplitude ratios down to -4 dB.

The distribution obtained from the azimuthal integration is a convolution of the transverse momentum distribution and the light intensity profile on the cathode. To recover the momentum distribution a Wiener filter approach will be used to deconvolve the measured distribution, approximating the light profile with a Gaussian point spread function.

## CONCLUSION

A dedicated UHV chamber for preparation and analysis of Alkali-Antimonide photocathodes has been developed. It allows in-situ characterisation of the cathodes using XPS, ion scattering, and the momentatron which yields the initial transverse momentum distribution of the photoelectrons. Details of the momentatron are presented and the relative accuracy of the momentum resolution is estimated to 3%. During the commissioning of the preparation chamber, a $Cs_3Sb$ cathode was grown and a QE of at least 0.5% is reported. The system will be moved to HZB in fall 2014 and it is intended to routinely prepare $K_2CsSb$ cathodes and investigate the influence of preparation parameters on structural properties of the cathode and its performance.

## ACKNOWLEDGMENT

## REFERENCES

[1] L. Cultrera et al. In: *APL* 103.10 (2013), p. 103504.

[2] J. Smedley et al. "K2CsSb Cathode Development." In: *AIP Conference Proceedings 1149, 18th International Spin Physics Symposium* (2009), pp. 1062–1066.

[3] S. G. Schubert et al., Proc. IPAC2014, MOPRI018, http://jacow.org/.

[4] H. A. Padmore. LBNL-ALS-LSBL 1124, 2012.

[5] Crytur.cz. Scintillation Materials Data Table.